

Growth differentiation factor 11 relieves acute lung injury in mice by inhibiting inflammation and apoptosis

H.-B. XU¹, B. QIN², J. ZHANG³, Y.-J. CHEN¹, W.-W. SHEN¹, L.-N. CAO⁴

¹Department of Emergency ICU, Caoxian People's Hospital, Heze, China

²Department of Surgery, Jinan Second Maternal and Child Health Hospital, Jinan, China

³Department of Obstetrics, Caoxian People's Hospital, Heze, China

⁴Department of Respiratory and Critical Medicine, Weifang Second People's Hospital, Weifang, China

Huabing Xu and Bo Qin contributed equally to this work

Abstract. – OBJECTIVE: Acute lung injury (ALI) is the most common organ damage in sepsis and sepsis-induced ALI is a clinically extremely dangerous disease. Therefore, it is essential to find an effective way to treat ALI. We hope to provide a new target for the treatment of clinical ALI by studying the effect of GDF11 on LPS-induced ALI.

MATERIALS AND METHODS: C57BL/6 male mice and lipopolysaccharide (LPS) were used to induce mouse ALI. Recombinant GDF11 protein was used to treat mice to detect the effect of GDF11 on mouse ALI. In addition, BEAS-2B cells were used to further validate the effects of GDF11 on inflammation and apoptosis of alveolar epithelial cells.

RESULTS: Recombinant GDF11 protein significantly reduced the expression of inflammatory factors and apoptosis-related pathways in mouse lung tissues. Overexpression of GDF11 in BEAS-2B cells also significantly attenuated the levels of inflammation and apoptosis in the cells. In addition, GDF11 can reduce the activity of TLR2/HMGB1/NF- κ B signaling pathway, which is an important mechanism for GDF11 to play a role in lung protection.

CONCLUSIONS: GDF11 can exert lung protection effects by inhibiting the TLR2/HMGB1/NF- κ B signaling pathway and reduce the level of inflammation and apoptosis of the lung.

Key Words:

Growth differentiation factor 11, Acute lung injury, Inflammation, Apoptosis, TLR2/HMGB1/NF- κ B.

Introduction

Sepsis is a complex systemic inflammatory response syndrome that can cause high mortality in critically ill patients and multiple organ fail-

ures, including the cardiovascular system, liver, kidneys, and lungs. Respiratory dysfunction is the most common complication of sepsis due to lung susceptibility. Sepsis-induced acute lung injury (ALI) is an important cause of death in clinical patients that threatens human health¹. Gram-positive bacterial infections are more common clinically. In the process of bacterial infection, the pathogenic components in the pathogen not only directly induce cell damage, but also cause severe inflammatory reactions leading to multiple tissue organ damage and organ failure². Therefore, inhibition of pulmonary inflammatory response caused by pathogenic factors is an effective means of treating ALI.

Growth Differentiation Factor 11 (GDF11) is one of the transforming growth factor- β (TGF- β) family. GDF11 is expressed in both embryonic and adult tissues³. In recent years, GDF11 has received much attention as an anti-aging factor, which has declined with age. Lee et al⁴ have shown that GDF11 can reverse aging and improve age-related muscle, nervous, and cardiovascular dysfunction. In a prospective cohort study, Olson et al⁵ found that in patients with stable ischemic heart disease, the higher the GDF11 level, the lower the risk of cardiovascular events and death. Animal experiments have shown that GDF11 can attenuate atherosclerosis in apolipoprotein E^{-/-} mice by improving endothelial dysfunction and reducing inflammation⁶. In our study, we found that GDF11 also plays an important role in sepsis-induced ALI. Lipopolysaccharide (LPS) was used to induce mouse ALI and we used recombinant GDF11 protein to detect the effect of GDF11 on mouse ALI. In addition, we cultured human normal lung epithelial cells to further verify the protective effect of GDF11 on the lungs.

Materials and Methods

Animals and Grouping

Thirty C56BL/6 male mice (8 weeks old, 18–22 g) were purchased from Beijing Charles River Experimental Animal Co., Ltd. (Beijing, China). Mice were housed in SPF barriers and fed with clean rat food and drinking water. We randomly divided mice into control group, ALI model group, and ALI model group plus drug-administered group. Recombinant mouse GDF11 (Amy-Jet, Wuhan, China) was used to subcutaneously inject mice. This study was approved by the Animal Ethics Committee of Caoxian People's Hospital.

Modeling of ALI

Mice were anesthetized with 4% chloral hydrate and placed in the supine position on the operating table. 75% ethanol was used to sterilize the neck of mice. After gently cutting the neck skin of the mouse with scissors, we used a vascular clamp to gently separate the muscles of the mouse neck until the trachea was exposed. We injected intratracheal injection of LPS (5 mg/kg; Sigma-Aldrich, St. Louis, MO, USA) into mice using a microsyringe. Moist rales in the lungs of mice indicated that LPS has been successfully injected into the trachea of mice. 24 h after the injection of LPS, we sacrificed mice and took the mouse serum and lung tissue for the next experiment.

Cell Culture and Treatment

We purchased human normal lung epithelial cell line, BEAS-2B cells (American Type Culture Collection (ATCC; Manassas, VA, USA)). Dulbecco's Modified Eagle's Medium/F12 (DMEM/F12) medium (Gibco, Rockville, MD, USA) was used to culture BEAS-2B cells and we added 10% fetal bovine serum (FBS; Gibco, Rockville, MD, USA) to DMEM/F12 medium to configure complete medium. All cell experiments were performed in a sterile clean bench.

Lentivirus Transfection

Lenti-NC and Lenti-GDF11 were built at Genekey Gene Biotechnology Co., Ltd. (Shanghai, China). After the cells were passaged to a 6-well plate, we added DMEM/F12 medium to the culture dish and placed in an incubator for cultivation. When the cell fusion reached 50–55%, we used Lipofectamine 3000 (Invitrogen, Carlsbad, CA, USA) to transfect the cells according to the instructions.

We divided the cells into four groups: control group, LPS group, LPS+Lenti-NC group, and LPS+Lenti-GDF11 group.

Western Blot Analysis

After processing the differently grouped cells, the cells were washed twice with phosphate-buffered saline (PBS) and 200 mL of radioimmuno-precipitation assay (RIPA) lysate (Invitrogen, Carlsbad, CA, USA) was added. After the cells were placed on ice for 15 min, we scraped the cells and transferred the lysate to the Eppendorf (EP) tube, and then we placed the EP tube again on ice for 15 min. The bicinchoninic acid (BCA) kit (Beyotime, Shanghai, China) was used to detect protein concentration. We added 5 x loading buffer (4:1) to the remaining protein solution and heated it to 100°C for 10 min. The protein was stored in a –80°C freezer. We performed sodium dodecyl sulphate-polyacrylamide gel electrophoresis (SDS-PAGE) electrophoresis with 50 µg of protein per well. Methanol was used to activate the polyvinylidene difluoride (PVDF) membrane (Millipore, Billerica, MA, USA). We then transferred the protein to the PVDF membrane at a constant flow of 280 mA. 5% skim milk was used to seal the PVDF membrane and then we used GDF11 antibody (Abcam, Cambridge, MA, USA) to incubate the PVDF membrane overnight at 4°C. After washing the PVDF membrane, we incubated it for 1 h at room temperature using secondary antibody (Abcam, Cambridge, MA, USA). Finally, we used chemiluminescent solution to detect protein bands.

RNA Isolation and Quantitative Real Time-Polymerase Chain Reaction (RT-PCR)

We took 20 mg of lung tissue from different mice and added 1 mL of TRIzol (Invitrogen, Carlsbad, CA, USA). We use an electric homogenizer for homogenization. We used a spectrophotometer to detect the concentration of extracted RNA. We reversed the RNA to complementary deoxyribose nucleic acid (cDNA) using SuperMix (Invitrogen, Carlsbad, CA, USA). We, then, amplified the cDNA using SYBR Green qPCR Master Mix (Invitrogen, Carlsbad, CA, USA). Primer sequences are shown in Table I.

Preparation of Bronchoalveolar Lavage Fluid (BALF)

At the end of the modeling, we took the mice and exposed the neck trachea of the mice. Then,

Table I. Primer sequences.

Name	sense/anti-sense	Sequence (5'-3')
Mouse		
IL-1 β	sense	GTTGACGTACTACGTACGTGATC
	anti-sense	AACGAGCATGCGGACTCTGCTAC
IL-6	sense	ACGACGTTCTACGTACGTACGTCT
	anti-sense	GCGTATCATGCGATCTCTGGTCA
IL-8	sense	AGCTCTTCCTCGAGCTGCATGCCA
	anti-sense	GCGCGCCGCGCATATGCAGCGTA
TNF- α	sense	ATCGTTCGAGCTTCAGCAGTCTGCA
	anti-sense	ATCCTGCCGCATATCTCAGTAGCA
caspase3	sense	CGCATGCTCTCAGCGTACGTACAT
	anti-sense	CTTCAGGACGTTGTGACCACGGTCA
caspase8	sense	ACGGTCAGTCGTACGTAGCTACGT
	anti-sense	AAGCTCGACTGACTGACGTAGT
caspase9	sense	GTCAGCGACGTACGTATCGAT
	anti-sense	ATCTCGTACGTGCTCTAGCGTA
Bax	sense	AATCTCGCGTACGTAGCTGCTA
	anti-sense	GGCTCTAAAGCTCTCAGAGTCT
Bcl-2	sense	GCCCTTAAGGCGTACTGACGT
	anti-sense	GCAACTTGAGCGCGTTCGAGCT
TLR2	sense	AGGTTCCGCACTATCGATGCG
	anti-sense	ACGATCTACCGCAATCGTACGT
HMGB1	sense	GGTCTCAAGCCGAATCCGAGCTC
	anti-sense	CTAAAGGCTACTGACGTCGGTT
NF- κ B p65	sense	AAGCTCTCGGCCCGGTAGCGTA
	anti-sense	CAGCCTTCGCACGATGCAGTCGTG
GAPDH	anti-sense	GGTTTCGACACCGTGTGGCATCGT
	anti-sense	AGCGCCCTTGGGGCTATCGACTA
Human		
IL-1 β	sense	ATCCCCTGTGGGCTATCAGTGTGT
	anti-sense	ACCTCGAGGGCTATCAGCACGTCA
IL-6	sense	GGTTCAAAGCGCTATACGTGTTCA
	anti-sense	GGTATTGCGTTCAGCGCGATCC
IL-8	sense	GTCTTTAGCAGACGGTCGTACCA
	anti-sense	GGTAGCTTCTAGCATCGTCAGTA
TNF- α	sense	TGGATTCCCAGAGATCTGAGACT
	anti-sense	ACCTGTAGCCCTTGGAGCAAC
GDF11	sense	GATTCGAGCGACGTACTACCA
	anti-sense	GGTCTTAAGCCGCTACACGTGTG
TLR2	sense	GGTTCAAAGCCGATCCGACGTGT
	anti-sense	AAGTCCCGAGCTACGTACGTGCA
HMGB1	sense	GTTCTAGCAGCCATCTCAGCGTGC
	anti-sense	TTCGAGCAGCAGTCACGTAGCCG
NF- κ B p65	sense	AGTCTTCGAGCGCATCGTAGCTC
	anti-sense	GGTCTCTAGCATGCTGACGTCGA
GAPDH	sense	GTCTACAGGCATGCAGTCAGA
	anti-sense	ACTTGGCACTTGCAGATCGTAC

we used a syringe to draw 0.5 mL of sterile saline for the tracheal injection of the mice. After gently shaking the mice, we re-suction saline with a syringe. After repeating three times, we collected BALF for further study. A cell counting plate was used to detect the total number of cells and the number of neutrophils in the BALF.

Enzyme-Linked Immunosorbent Assay (ELISA)

We collected BALF from mice or cell culture supernatant and centrifuged to remove impurities. Each group of BALF was sequentially added to a 96-well plate and placed in a 37°C incubator

for 2 h. We then used ELISA kits (R&D Systems, Minneapolis, MN, USA) to detect concentrations of IL-1 β , IL-6, IL-8, and TNF- α in BALF or serum, respectively.

Hematoxylin and Eosin (HE) Staining

Immediately after obtaining mouse lung tissue, we placed the lung tissue in formaldehyde for 24 h and made paraffin blocks. After making paraffin sections using a microtome, we dewaxed and hydrated the paraffin sections and performed HE staining. Hematoxylin (Solarbio, Beijing, China) was used to incubate paraffin sections for 5 min. After washing the paraffin sections, the eosin solution (Solarbio, Beijing, China) was used to incubate the paraffin sections for 3 min. We then washed the paraffin sections with gradient ethanol and sealed them with neutral gum.

Immunohistochemical (IHC) Staining

After dewaxing and hydrating the paraffin sections, we placed the paraffin sections in pH 6.0 citrate buffer for antigen retrieval. Next, we incubated for 20 min at room temperature using peroxidase blocker. After washing paraffin sections with PBS, the paraffin sections were soaked with goat serum for 1 h and incubated with primary antibody (Abcam, Cambridge, MA, USA) for 4°C overnight. Then, after washing the paraffin sections with PBS, we incubated them for 2 h at room temperature using the universal secondary antibody in the immunohistochemistry kit (Thermo Fisher Scientific, Waltham, MA, USA). Finally, we use color developer for color development.

Immunofluorescence (IF) Staining

After treating the differently grouped cells, we took the cells and discarded the medium. We then fixed it with paraformaldehyde for 20 min and blocked with 5% bovine serum albumin (BSA) for 30 min. We then incubated with primary antibody (Abcam, Cambridge, MA, USA) overnight at 4°C. After washing the cells with PBS, the fluorescent secondary antibody (Abcam, Cambridge, MA, USA) was added to the cells and incubated for 1 h at room temperature. Then, we added 4',6-diamidino-2-phenylindole (DAPI) to stain the nucleus. After washing with PBS, we observed and photographed (200 \times) using a fluorescence microscope (Leica IL LED, Wetzlar, Germany).

Cell Apoptosis Detection

We used the Annexin V/PI kit (Genechem, Shanghai, China) to detect apoptosis. After passage of the cells to 6-well plates, we transfected or stimulated the cells. We collected each group of cells and washed them twice with PBS. Next, we suspended the cells with 400 μ L of Annexin V binding solution and added 5 μ L of Annexin V-FITC staining solution. After incubating for 15 min in the dark, we added 10 μ L of PI staining solution and continued to incubate at 4°C for 5 min in the dark. Then, we used a flow cytometer to detect the apoptotic rate. The detection of apoptosis in mouse lung tissue is similar to that of cells.

Statistical Analysis

Statistical Product and Service Solutions (SPSS) 21.0 statistical software (IBM, Armonk, NY, USA) and GraphPad prism 7.0 software (La Jolla, CA, USA) were used for data analysis and processing in this study. Experimental data are expressed as mean \pm standard deviation. Comparison between multiple groups was done using One-way ANOVA test followed by Post-Hoc Test (Least Significant Difference). Pairwise comparisons were performed using the Student-Newman-Keuls (SNK) method. $p < 0.05$ indicates that the difference was statistically significant. All experiments were repeated 3 times.

Results

Recombinant Mouse GDF11 Attenuates LPS-Induced Lung Inflammatory Response In Mice

To demonstrate the anti-inflammatory effects of recombinant GDF11 protein on mouse lung tissue, we injected subcutaneously recombinant GDF11 100 μ g/kg in ALI mice. We took mouse BALF and examined the number of cells in BALF. The results showed that the total number of cells and the number of neutrophils in the BALF of LPS group were significantly increased, while GDF11 could reduce their number (Figure 1A, 1B). In addition, ELISA (Figure 1C) detected the expression of inflammatory factors in BALF and the results indicated that GDF11 significantly reduced the expression of IL-1 β , IL-6, IL-8, and TNF- α . The results of RT-PCR (Figure 1D) were similar to ELISA. HE staining (Figure 1E) examined the morphology of mouse lung tissue and the results showed that LPS-induced lung

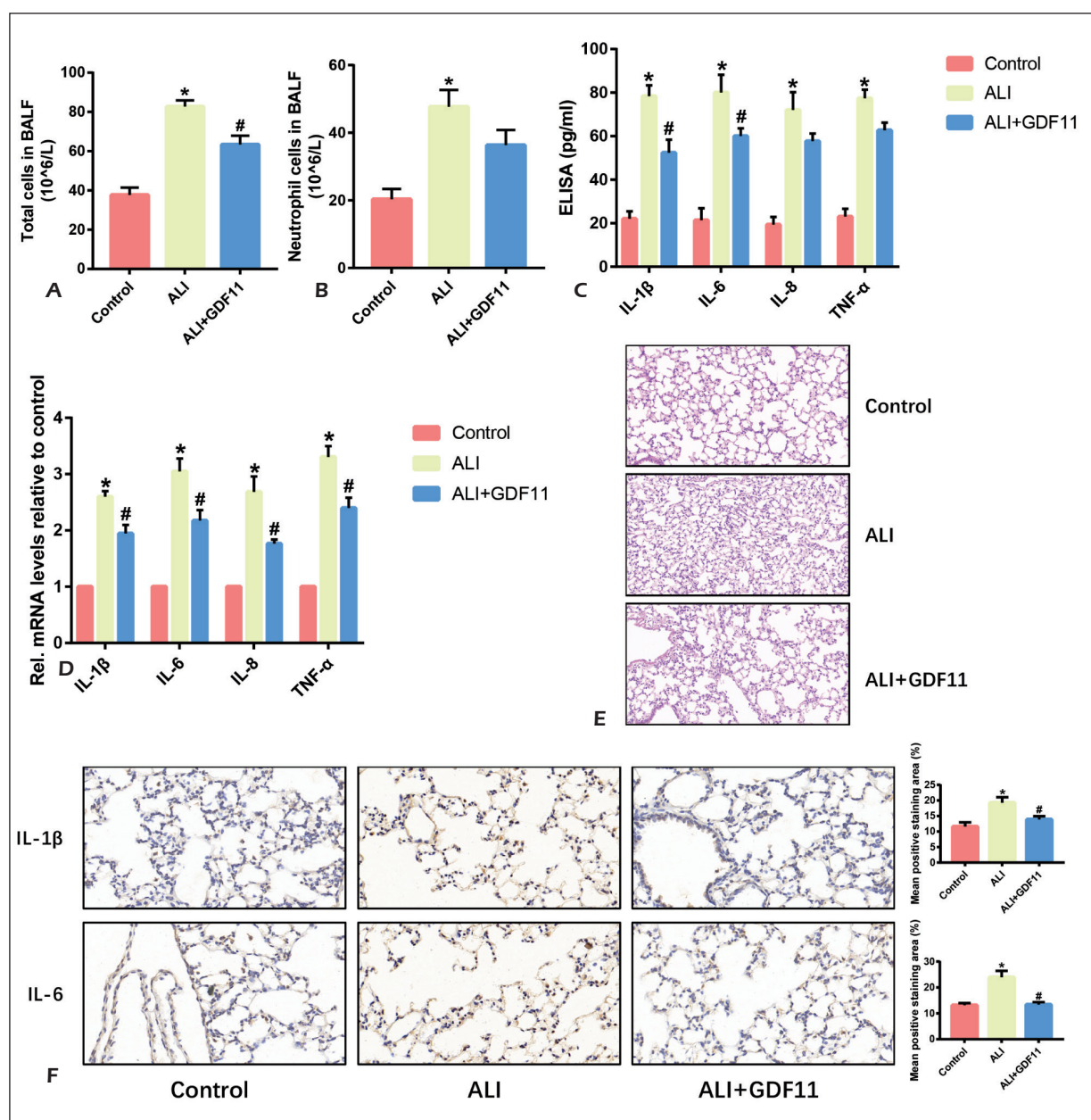


Figure 1. Recombinant mouse GDF11 attenuates LPS-induced lung inflammatory response in mice. **A-B**, Total cells number (**A**) and neutrophil cells number (**B**) in BALF were detected. **C**, ELISA detected the content of IL-1 β , IL-6, IL-8 and TNF- α in BALF. **D**, Expression of IL-1 β , IL-6, IL-8 and TNF- α in mice lung tissue was also detected by RT-PCR. **E**, HE staining detected the effect of GDF11 on lung morphology (magnification: 200 \times). **F**, IHC staining detected the expression of IL-1 β and TNF- α (magnification: 200 \times). (“*” means $p < 0.05$ vs. the control group and “#” means $p < 0.05$ vs. the ALI group).

tissue showed morphological disorder in mice and inflammatory cell infiltration in the pulmonary interstitial, while GDF11 can improve the morphology of lung tissue. IHC staining (Figure 1F) detected the expression of IL-1 β and IL-6 in mouse lung tissues and the results indicated that GDF11 effectively reduced the level of inflammation in mouse lung tissue.

Recombinant Mouse GDF11 Reduces Apoptosis In Mouse Lung Tissue

We treated mice with recombinant GDF11 protein and detected changes in the level of apoptosis in mouse lung tissue. The results of IHC staining (Figure 2A) showed that the apoptosis level of lung tissue in LPS-induced mice was significantly increased, showing an increase in caspase3 and

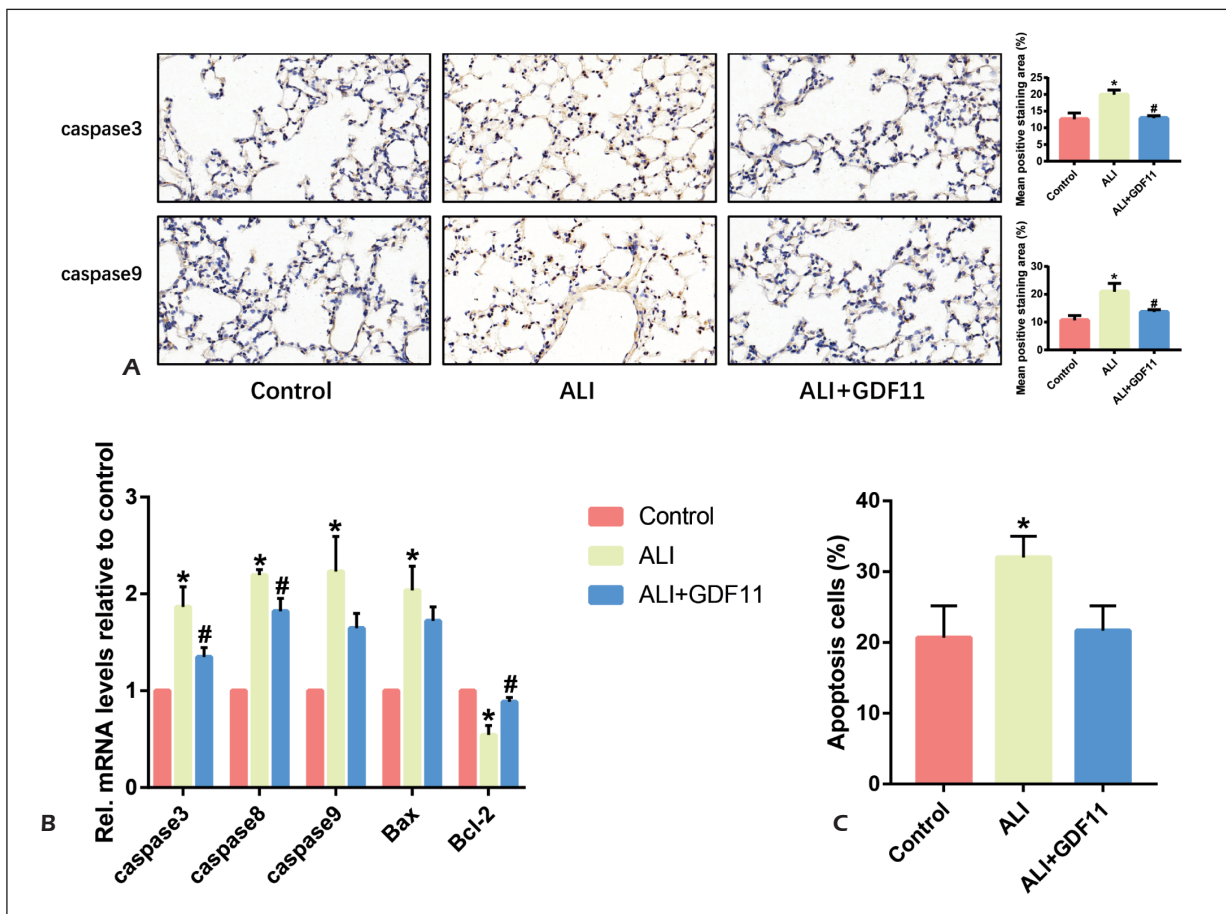


Figure 2. Recombinant mouse GDF11 reduces apoptosis in mouse lung tissue. **A**, Expression of caspase3 and caspase9 was determined by IHC staining (magnification: 200×). **B**, RT-PCR detected the expression of caspase3, caspase8, caspase9, Bax, and Bcl-2. **C**, Apoptosis rate of lung tissue in mice was determined by flow cytometry. (“*” means $p < 0.05$ vs. the control group and “#” means $p < 0.05$ vs. the ALI group).

caspase9, and recombinant GDF11 protein could reduce their expression. In addition, RT-PCR (Figure 2B) results also showed that GDF11 can decrease the expression of caspase3, caspase8, caspase9, and Bax and increase the expression of Bcl-2. Flow cytometry (Figure 2C) detected the apoptotic rate of mouse lung tissue and the results showed that GDF11 significantly reduced the apoptotic rate.

Overexpression of GDF11 Attenuates LPS-Induced Damage to BEAS-2B Cells

To further validate the effect of GDF11 on alveolar epithelium, we used lentiviral transfection to increase the expression of GDF11 in BEAS-2B cells. The efficiency of lentiviral transfection was detected by Western blot (Figure 3A) and RT-PCR (Figure 3B). LPS (0.5 μg/mL) was used to induce BEAS-2B cell damage. Changes in cellular inflammatory levels were examined by ELISA (Figure

3C) and RT-PCR (Figure 3D) and the results indicate that overexpression of GDF11 significantly reduces the expression of inflammatory factors. IF staining (Figure 3E, 3F) detected the expression of caspase3 and caspase9 in BEAS-2B cells and the results indicated that overexpression of GDF11 significantly reduced their expression. The results of RT-PCR (Figure 3G) also demonstrated the anti-apoptotic effect of GDF11. The results of flow cytometry (Figure 3H) indicated that overexpression of GDF11 reduced the rate of apoptosis.

GDF11 Inhibits the TLR2/HMGB1/NF-κB Signaling Pathway In Mouse Lung Tissue and BEAS-2B Cells

We examined the effect of GDF11 on the TLR2/HMGB1/NF-κB signaling pathway. The results of IHC staining (Figure 4A) and RT-PCR (Figure 4B) in mouse lung tissue showed that the activity of TLR2/HMGB1/NF-κB signaling pathway was significantly

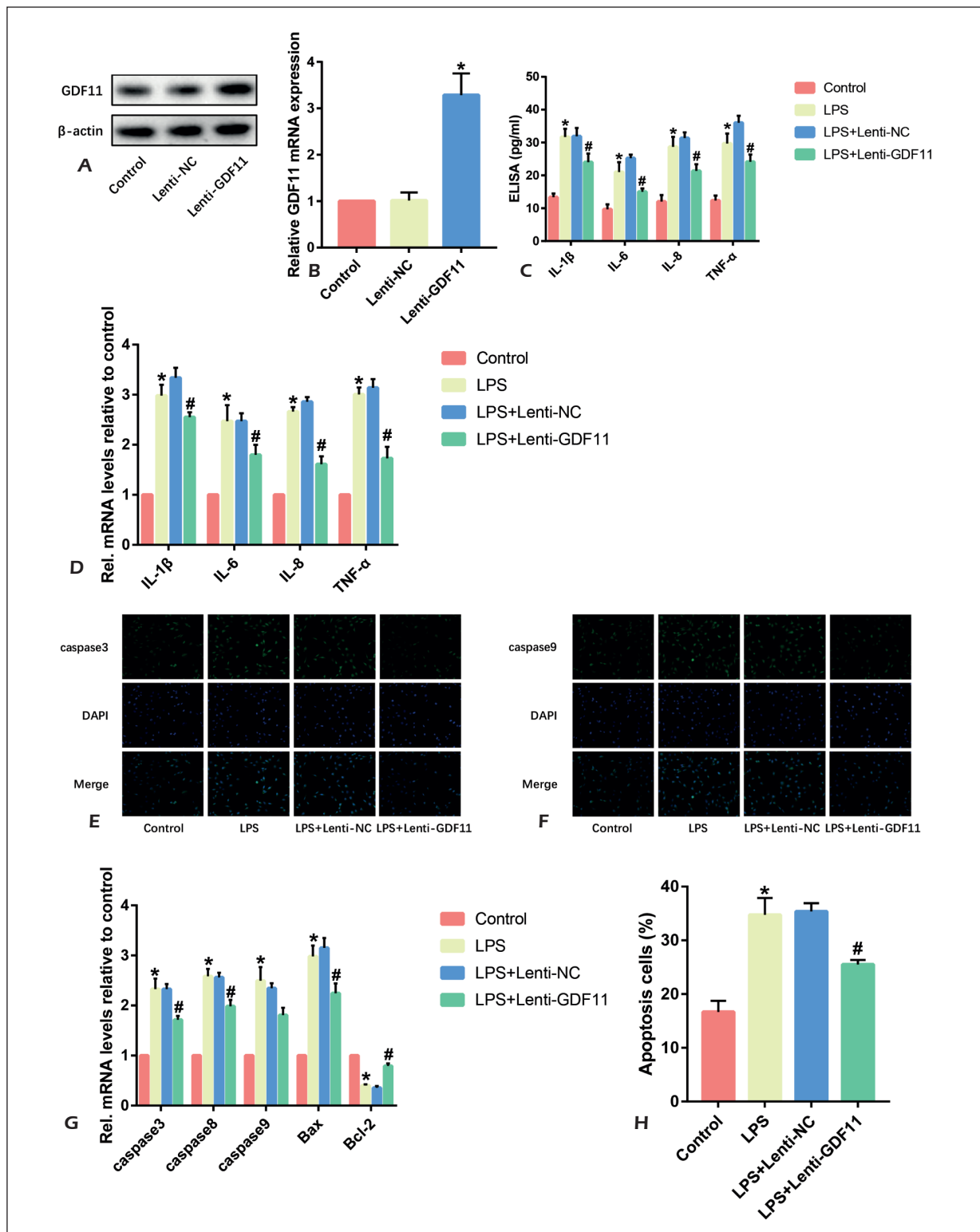


Figure 3. Overexpression of GDF11 attenuates LPS-induced damage to BEAS-2B cells. **A-B**, Transfection efficiency of Lenti-GDF11 was determined by western blot (**A**) and RT-PCR (**B**). **C-D**, Expression of IL-1 β , IL-6, IL-8 and TNF- α in BEAS-2B cells was determined by ELISA (**C**) and RT-PCR (**D**). **E-F**, IF staining detected the expression of caspase3 and caspase9 (magnification: 200 \times). **G**, RT-PCR detected the expression of caspase3, caspase8, caspase9, Bax and Bcl-2. **H**, Apoptosis rate of lung tissue in BEAS-2B cells was determined by flow cytometry. (“*” means $p < 0.05$ vs. the control group and “#” means $p < 0.05$ vs. the LPS+Lenti-NC group).

increased in LPS-induced lung tissue of mice, while recombinant GDF11 protein reduced expression of TLR2, HMGB1, and NF-κB p65. In cell experiments, overexpression of GDF11 also significantly reduced the activity of the TLR2/HMGB1/NF-κB signaling pathway in BEAS-2B cells (Figure 4C-4E).

Discussion

An inflammatory cascade triggered by ALI involves activating inflammatory cells and stimulating their releasing mediators⁷. Proinflammatory cytokines (such as IL-1β, TNF-α, IL-6 or IL-8)

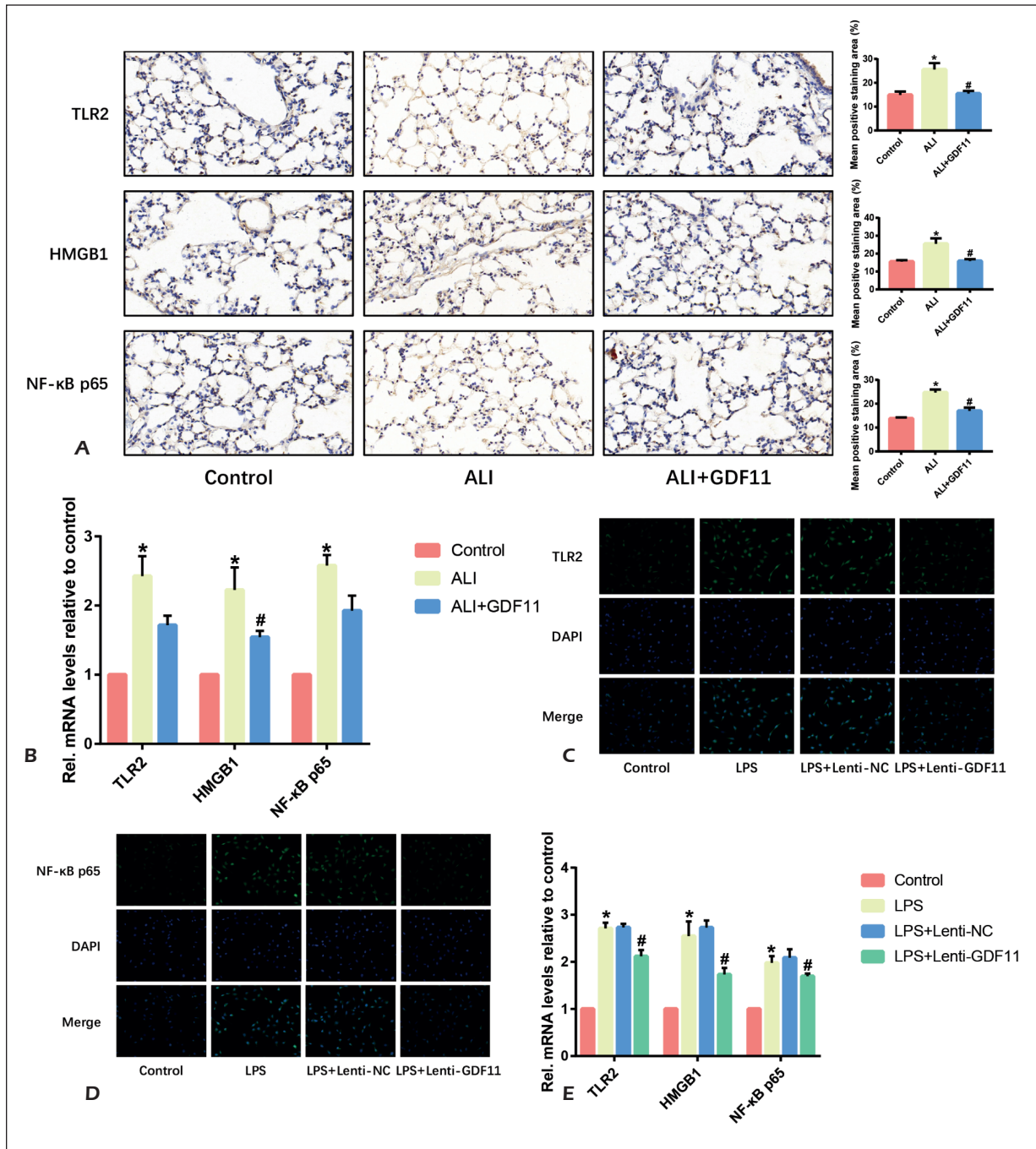


Figure 4. GDF11 inhibits the TLR2/HMGB1/NF-κB signaling pathway in mouse lung tissue and BEAS-2B cells. **A-B**, IHC staining (**A**) (magnification: 200×) and RT-PCR (**B**) detected the expression of TLR2, HMGB1 and NF-κB p65 in lung tissue. **C-E**, IF staining (**C-D**) (magnification: 200×) and RT-PCR (**E**) detected the expression of TLR2, HMGB1 and NF-κB p65 in BEAS-2B cells. (“*” means $p < 0.05$ vs. the control group and “#” means $p < 0.05$ vs. the ALI group or LPS+Lenti-NC group)

and anti-inflammatory cytokines (such as IL-10, IL-13) may be detected in serum or in BALF, which is mainly caused by the release of cells or dead cells recruited into the alveolar space. Cytokines activate neutrophils to adhere to the capillary endothelial surface of capillaries and migrate into the stroma and alveoli⁸. Activated neutrophils release more cytokines and act as signaling molecules, playing a key role in initiation, amplification, sustained local and systemic inflammation. Zhang et al⁹ have shown that lung tissue damage in ALI may be related to the effects of inflammatory mediator release on normal cell apoptosis during inflammatory reactions. Under pathological conditions, Fas/FasL binding directly leads to tissue cell apoptosis. It was observed in *in vitro* cell culture that Fas was expressed on the surface of both pulmonary vascular endothelial cells and lung epithelial cells, but the number was normally small, and the expression of Fas was increased after stimulation with inflammatory factors such as LPS. Fas expression was increased on the surface of the lung epithelium in patients with ALI, and a large amount of FasL was also detected in the pulmonary edema fluid. The death patient has higher FasL content, leading to apoptosis of normal lung epithelial cells. This phenomenon can be blocked by specific inhibitors of FasL. A large number of animals and *in vitro* experiments have also demonstrated that activation of the Fas/FasL pathway leads to apoptosis of lung epithelial cells and lung injury. Herrero et al¹⁰ have shown that after administration of anti-Fas antibodies and recombinant human soluble Fas ligand (rh-sFasL) in experimental animals, apoptosis of lung epithelial cells precedes neutrophil infiltration, and these phenomena are attenuated in Fas and FasL knockout mice. Our study found that recombinant mouse GDF11 protein effectively reduced the number of neutrophils and inflammatory factors in BALF. In addition, GDF11 also significantly reduced the level of apoptosis in mouse lung tissue, manifested by a decrease in caspase3, caspase8 and caspase9 and an increase in the ratio of Bcl-2/Bax. In cell experiments, overexpression of GDF11 also showed significant protection against BEAS-2B cells and reduced levels of inflammation and apoptosis in BEAS-2B cells.

The innate immune system recognizes and resists pathogen infection or maintains homeostasis after infection through pathogen recognition receptors (PRRs) and binds pathogen-associated molecular patterns (PAMPs). Toll-like receptor 4 (TLR4) is the earliest discovered PRR that recog-

nizes LPS on the surface of Gram-negative bacteria. This identification method is formed by the long-term evolution of organisms, helping organisms to recognize the infection of foreign bacteria and building a bridge between the body's immune system and the external microbial system¹¹. At present, there are more than a dozen TLRs that can recognize various *in vitro* and *in vivo* pathogenic components such as bacteria, viruses, LPS, DNA, and RNA¹². TLR2 is one of the PRRs. It is well known that TLR2 can be activated by lipoteichoic acid (LTA) to further activate adapter molecules in the Toll/IL-1 receptor (TIR) domain, including myeloid differentiation primary-response protein 88 (MyD88), TIR-domain-containing adapter-inducing interferon (TRIF), and TRIF-related adaptor molecular (TRAM)¹³. The recruitment of these receptor molecules to TLR2 triggers different signal transduction and forms signal-activated complexes, including ubiquitination of tumor necrosis factor receptor associated factor 6 (TRAF6) and phosphorylation of transforming growth factor beta-activated kinase 1 (TAK1), thereby activating MAPK (p38MAPK, ERK, and JNK) and NF- κ B signaling pathways¹⁴. The MPAK signaling pathway is a cascade of enzymatic reactions consisting of MAPKKK, MAPKK, and MAPK, amplifying the binding signals from LTA and TLR2, and finally activating transcription factors such as cAMP response element binding protein (CREB) and activator protein 1 (AP1)¹⁵. The NF- κ B signaling pathway is another inflammatory activation pathway that activates I κ B α by upstream IKK α and IKK β to promote ubiquitination and degradation of I κ B α , thereby releasing p65 and p50 molecules into the nucleus and involved in transcriptional activity regulation. MAPK signaling pathway and NF- κ B signaling pathway are important signaling pathways mediated by TLRs, promote transcription factor activation and promote the production of cytokines and chemokines. A large amount of aggregation of cytokines promotes the expression of TNF- α , IL-6, and IL-1 β , leading to the occurrence of sepsis in the body. The pro-inflammatory factor TNF- α not only directly induces apoptosis in lung epithelial cells and endothelial cells, but also activates other immune cells¹⁶. IL-1 β and IL-6 can up-regulate the body's temperature regulation center and cause high fever. Therefore, blocking TLR2-mediated signaling pathways (NF- κ B and MAPK) may be an effective strategy for the treatment of ALI induced by Gram-positive bacteria¹⁷.

HMGB1 is one of the alarm proteins and plays a key role in the early antigen presentation and activation of cells in immune responses¹⁸. In an animal model of arthritis, HMGB1 promotes inflammatory responses via receptor pathways such as TLR2, TLR4, and advanced glycation end products receptor (RAGE), and the content of HMGB1 and disease severity is closely related¹⁹. HMGB1 has been studied in sepsis as a late inflammatory mediator. Under the stimulation of LPS, HMGB1 can be redistributed from the nucleus to the cytoplasm, and play a role in pro-inflammatory cytokines. In the plasma and lung epithelial stroma of ALI mice induced by LPS, HMGB1 levels were detected to be significantly elevated. It can cause acute lung inflammation and is characterized by neutrophil infiltration, alveolar congestion, and pulmonary hemorrhage. The concentration of HMGB1 can reflect the severity of inflammation and tissue damage and is closely related to the prognosis of the disease²⁰. Anti-HMGB1 antibodies attenuate endotoxin-induced lung injury. When extracellular HMGB1 binds to cell surface receptors such as TLR2, TLR4, and RAGE, it leads to NF- κ B and MAPK activation. In this activation process, macrophages can be used as target cells to produce pro-inflammatory factors such as TNF- α , IL-1 β , IL-6, and macrophage inflammatory protein, and the inflammatory mediators such as TNF- α , IL-1 β and RAGE can positively promote the expression of HMGB1²¹. Therefore, HMGB1 may provide a new therapeutic target for the cascade amplification reaction that blocks the inflammatory pathway.

In our study of ALI, we found that HMGB1/TLR2/NF- κ B signaling pathway is significantly elevated in LPS-induced lung and BEAS-2B cells. This may be an important mechanism for GDF11 to protect lung. Therefore, GDF11 has a good application prospect in the treatment of ALI. We hope that this research will provide new targets for the treatment of clinical ALI.

Conclusions

Altogether, these findings showed that recombinant GDF11 protein significantly reduced the level of inflammation and apoptosis in lung tissue of ALI mice. In addition, overexpression of GDF11 reduced the levels of inflammation and apoptosis in BEAS-2B cells. TLR2/HMGB1/NF- κ B signaling pathway is an important mechanism of LPS-induced ALI, and GDF11 has a significant inhibitory effect on TLR2/HMGB1/NF- κ B signaling pathway.

Conflict of Interests

The authors declared that they have no conflict of interests.

References

- 1) FAUST HE, REILLY JP, ANDERSON BJ, ITTNER CAG, FORKER CM, ZHANG P, WEAVER BA, HOLENA DN, LANKEN PN, CHRISTIE JD, MEYER NJ, MANGALMURTI NS, SHASHATY MGS. Plasma mitochondrial DNA levels are associated with acute respiratory distress syndrome in trauma and sepsis patients. *Chest* 2019 Oct 14. pii: S0012-3692(19)34010-3. doi: 10.1016/j.chest.2019.09.028. [Epub ahead of print]
- 2) WANG YM, JI R, CHEN WW, HUANG SW, ZHENG YJ, YANG ZT, QU HP, CHEN H, MAO EQ, CHEN Y, CHEN EZ. Paclitaxel alleviated sepsis-induced acute lung injury by activating MUC1 and suppressing TLR-4/NF-kappaB pathway. *Drug Des Devel Ther* 2019; 13: 3391-3404.
- 3) FANG Z, ZHU Z, ZHANG H, PENG Y, LIU J, LU H, LI J, LIANG L, XIA S, WANG Q, FU B, WU K, ZHANG L, GINZBURG Y, LIU J, CHEN H. GDF11 contributes to hepatic HAMP inhibition through SMURF1-mediated BMP-SMAD signalling suppression. *Br J Haematol* 2019 Aug 16. doi: 10.1111/bjh.16156. [Epub ahead of print]
- 4) LEE M, OIKAWA S, USHIDA T, SUZUKI K, AKIMOTO T. Effects of exercise training on growth and differentiation factor 11 expression in aged mice. *Front Physiol* 2019; 10: 970.
- 5) OLSON KA, BEATTY AL, HEIDECKER B, REGAN MC, BRODY EN, FOREMAN T, KATO S, MEHLER RE, SINGER BS, HVEEM K, DALEN H, STERLING DG, LAWN RM, SCHILLER NB, WILLIAMS SA, WHOOLEY MA, GANZ P. Association of growth differentiation factor 11/8, putative anti-ageing factor, with cardiovascular outcomes and overall mortality in humans: analysis of the Heart and Soul and HUNT3 cohorts. *Eur Heart J* 2015; 36: 3426-3434.
- 6) ZHAO L, ZHANG S, CUI J, HUANG W, WANG J, SU F, CHEN N, GONG Q. TERT assists GDF11 to rejuvenate senescent VEGFR2(+)/CD133(+) cells in elderly patients with myocardial infarction. *Lab Invest* 2019; 99: 1661-1688.
- 7) LIANG WJ, ZENG XY, JIANG SL, TAN HY, YAN MY, YANG HZ. Long non-coding RNA MALAT1 sponges miR-149 to promote inflammatory responses of LPS-induced acute lung injury by targeting MyD88. *Cell Biol Int* 2019 Sep 9. doi: 10.1002/cbin.11235. [Epub ahead of print]
- 8) LIN CK, LIN YH, HUANG TC, SHI CS, YANG CT, YANG YL. VEGF mediates fat embolism-induced acute lung injury via VEGF receptor 2 and the MAPK cascade. *Sci Rep* 2019; 9: 11713.
- 9) ZHANG Y, HUANG T, JIANG L, GAO J, YU D, GE Y, LIN S. MCP-induced protein 1 attenuates sepsis-induced acute lung injury by modulating macrophage polarization via the JNK/c-Myc pathway. *Int Immunopharmacol* 2019; 75: 105741.
- 10) HERRERO R, PRADOS L, FERRUERO A, PUIG F, PANDOLFI R, GUILLAMAT-PRATS R, MORENO L, MATUTE-BELLO G,

- ARTIGAS A, ESTEBAN A, LORENTE JA. Fas activation alters tight junction proteins in acute lung injury. *Thorax* 2019; 74: 69-82.
- 11) MAHER DP, WALIA D, HELLER NM. Morphine decreases the function of primary human natural killer cells by both TLR4 and opioid receptor signaling. *Brain Behav Immun* 2020; 83: 298-302.
 - 12) DO NASCIMENTO XAVIER BM, FERREIRA LAMP, FERREIRA LKDP, GADELHA FAAF, MONTEIRO TM, DE ARAÚJO SILVA LA, RODRIGUES LC, PIUVEZAM MR. MHTP, a synthetic tetratetrahydroisoquinoline alkaloid, attenuates lipopolysaccharide-induced acute lung injury via p38MAPK/p65NF-kappaB signaling pathway-TLR4 dependent. *Inflamm Res* 2019; 68: 1061-1070.
 - 13) LEE HR, SHIN SH, KIM JH, SOHN KY, YOON SY, KIM JW. 1-palmitoyl-2-linoleoyl-3-acetyl-rac-glycerol (PLAG) rapidly resolves LPS-induced acute lung injury through the effective control of neutrophil recruitment. *Front Immunol* 2019; 10: 2177.
 - 14) LI XQ, LV HW, TAN WF, FANG B, WANG H, MA H. Role of the TLR4 pathway in blood-spinal cord barrier dysfunction during the bimodal stage after ischemia/reperfusion injury in rats. *J Neuroinflammation* 2014; 11: 62.
 - 15) MURPHY M, XIONG Y, PATTABIRAMAN G, QIU F, MEDVEDEV AE. Pellino-1 positively regulates Toll-like Receptor (TLR) 2 and TLR4 signaling and is suppressed upon induction of endotoxin tolerance. *J Biol Chem* 2015; 290: 19218-19232.
 - 16) LYU Y, JIA S, WANG S, WANG T, TIAN W, CHEN G. Gestational diabetes mellitus affects odontoblastic differentiation of dental papilla cells via Toll-like receptor 4 signaling in offspring. *J Cell Physiol* 2019 Oct 9. doi: 10.1002/jcp.29240. [Epub ahead of print]
 - 17) TIAN H, LIU Z, PU Y, BAO Y. Immunomodulatory effects exerted by Poria Cocos polysaccharides via TLR4/TRAF6/NF-kappaB signaling in vitro and in vivo. *Biomed Pharmacother* 2019; 112: 108709.
 - 18) LIU Y, CHEN P, XU L, OUYANG M, WANG D, TANG D, YANG L, XIE M, CAO L, YANG M. Extracellular HMGB1 prevents necroptosis in acute myeloid leukemia cells. *Biomed Pharmacother* 2019; 112: 108714.
 - 19) XU Y, SHEN J, RAN Z. Emerging views of mitophagy in immunity and autoimmune diseases. *Autophagy* 2019 Apr 5:1-15. doi: 10.1080/15548627.2019.1603547. [Epub ahead of print].
 - 20) SANTILLO A, FIGLIOLA L, CAROPRESE M, MARINO R, D'APOLITO M, GIARDINO I, ALBENZIO M. Effect of lipid fraction of digested milk from different sources in mature 3T3-L1 adipocyte. *J Dairy Res* 2019; 86: 129-133.
 - 21) IM KI, NAM YS, KIM N, SONG Y, LEE ES, LIM JY, JEON YW, CHO SG. Regulation of HMGB1 release protects chemoradiotherapy-associated mucositis. *Mucosal Immunol* 2019; 12: 1070-1081.